2020-01-0536 Published 14 Apr 2020

Bake Hardening Behavior of DP, TBF, and PHS Steels with Ultimate Tensile Strengths Exceeding 1 GPa

Brandon W. Blesi, Charles Smith, David K. Matlock, and Emmanuel De Moor Colorado School of Mines

Citation: Blesi, B.W., Smith, C., Matlock, D.K., and De Moor, E., "Bake Hardening Behavior of DP, TBF, and PHS Steels with Ultimate Tensile Strengths Exceeding 1 GPa," SAE Technical Paper 2020-01-0536, 2020, doi:10.4271/2020-01-0536.

Abstract

Third generation advanced high strength steels (AHSS) have been developed combining high strength and formability, allowing for lightweighting of vehicle structural components. These AHSS components are exposed to paint baking operations ranging in time and temperature to cure the applied paint. The paint baking treatment, combined with straining induced from part forming, may lead to increased in-service component performance due to a strengthening mechanism known as *bake hardening*. This study aims to quantify the bake hardening behavior of select AHSS grades. Materials investigated were press hardenable steels (PHS) 1500 and 2000; transformation induced plasticity (TRIP) aided bainitic ferrite (TBF) 1000 and 1200; and dual phase (DP) 1000. The number designations of these grades refer to minimum as-received ultimate tensile strengths in MPa. Paint baking was simulated using industrially relevant times and temperatures from 15 to 60 min and 120 to 200 °C, respectively. Samples were prestrained 0, 2, or 5 pct to replicate part forming. Bake hardening values ranging from 90 to 140 MPa were observed for DP and TBF grades that were prestrained 2 pct and baked at 170 °C for 20 min. However, ductility diminished for these steels when subjected to 5 pct prestrain with uniform elongations after baking decreasing to 1 pct in some instances. PHS steels, on the other hand, showed substantial increases in yield strength without prestrain. Increases of 122 and 175 MPa were recorded for PHS 1500 and PHS 2000, respectively, following baking at 160 °C for 60 min. However, ultimate tensile strengths decreased due to reduced strain hardening, while total elongations decreased slightly.

1. Introduction

Current automotive safety and fuel efficiency standards put in place in the last decade have challenged original equipment manufacturers (OEMs) to continuously improve vehicle performance. For example, the National Highway Traffic Safety Administration (NHTSA) and the Environmental Protection Agency (EPA) have published Corporate Average Fuel Economy (CAFE) standards requiring passenger cars and light trucks manufactured in model years 2017 through 2025 to have an average fleet-wide fuel economy of 40.3-41.0 mpg by 2021 (phase I) and 49.7 mpg by 2025 (phase II) [1]. Advanced materials are essential for improving fuel efficiency and maintaining strict safety standards by producing lightweight, high strength parts. Weight reduction is possible via down-gauging of sheet metal components, which necessarily requires an increase in strength of the metal.

Sheet forming processes used to create structural members for a body-in-white (BIW) and subsequent paint baking operations strengthen steels via static strain aging mechanisms and is also referred to as *bake hardening* (BH). Paint baking (time and temperature) used to cure coatings can have a substantial effect on the mechanical properties of sheet steels in addition to the amount of plastic strain induced during forming. Solute redistribution and/or alteration in microstructure in certain steel grades after paint baking can create a noteworthy increase in tensile yield strength, which may lead to increased dent resistance and crashworthiness of automobiles.

Strain aging and bake hardening have been investigated over the course of several decades for numerous steel microstructures, ranging from ultra-low carbon (ULC) ferrite to multiphase steels, at various strength levels. Strain aging theory was originally proposed by Cottrell and Bilby [2] who first considered general solute effects: the interaction between the stress field produced by a solute atom and a dislocation. The elastic strain energy produced by lattice distortion from solute atoms is minimized by the strain energy of a dislocation creating a driving force for atom diffusion to dislocation cores. The diffusion of interstitial atoms (*e.g.* carbon, nitrogen) to dislocation cores is known as *Cottrell atmosphere formation*. Like any diffusional process, strain aging is time and temperature dependent. Other involved strengthening mechanisms, as summarized by Matlock et al. [3], include Snoek reordering and carbide precipitation.

More recent developments have focused on the bake hardening behavior of high strength dual phase (DP) steels. Waterschoot et al. [4] investigated strain aging in DP steels having different microstructures and strengths. These authors related increases in strengthening as a function of aging time to three distinct stages: (1) the pinning stage - dislocations in

ferrite are pinned by interstitial carbon resulting in an increase in strength of about 30 MPa, (2) precipitation stage - excess carbon forms carbon clusters or transition carbides with a maximum observed strengthening of 65 MPa, and (3) martensite tempering - internal stresses in ferrite from martensite transformation are reduced due to volume decrease of martensite and formation of transition carbides leading to large increases in strength between 160 and 250 MPa. Timokhana et al. [5,6] used transmission electron microscopy (TEM) and atom probe tomography (APT) to show that the increased dislocation density near the ferrite-martensite interface, likely due to stress propagation into ductile ferrite during martensite transformation, is a significant contributing factor to the pronounced BH response of DP steels. They also observed rod-like carbide formation in martensite after BH, confirming martensite tempering.

Other researchers have investigated the influence of prestrain, aging time and temperature, martensite morphology and phase fraction, and strength levels on the BH of DP steels [7, 8, 9, 10, 11]. Gündüz et al. [7,8] showed that increasing prestrain from 2 to 4 pct decreased the extent of strengthening after paint baking. These authors also showed that it is possible to "overage" DP steels for temperatures at and above 200 °C for 30 min, which results in a decrease in strengthening due to tempering of martensite and coarsening of precipitates. They found that the overaging process was suppressed in a microalloyed DP steel. Türkmen et al. [9] showed that fibrous (*i.e.* fine, needle-like lath) martensite uniformly distributed in ferrite, compared to blocky martensite, leads to higher strengthening because proportionally more regions of ferrite contain higher dislocation densities. Overaging was also found to be slower in fibrous martensite. These researchers showed that a larger martensite volume fraction led to greater BH values due to stronger dislocation pinning at ferrite-martensite interfaces. Ji et al. [10] investigated the BH response of DP steels with varying strengths, with the greatest level approaching 1 GPa. They observed that the higher strength microstructures with higher volume fractions of martensite, smaller martensite islands, and smaller ferrite grains produced the highest BH response. Ramazani et al. [11] showed for a DP 600 steel that large BH responses without prestrain are possible due to the generation of mobile geometrically necessary dislocations (GNDs) at the ferrite-martensite interface during processing. They also showed that the maximum strengthening of 80 MPa was observed at 2 pct prestrain and at temperatures at or below 170 °C. Strengthening decreased at higher prestrains and at higher temperatures due to overaging effects.

The microstructures of transformation induced plasticity (TRIP)-type steels are more complex than DP steels making determination of the fundamental BH mechanisms more difficult. Samek et al. [12] studied the BH response of TRIP steels by first considering the BH of individual microstructures. Ferrite and bainite microstructures were produced in bulk with adjusted chemistries to reflect the chemistry of each microstructure observed in a TRIP steel, and their strained and unstrained (*i.e.* 0 pct prestrain) response measured. They found that, like DP steels, the static strain aging of ferrite is due to Cottrell atmosphere formation and reduction in internal stresses produced by the austenite-to-martensite transformation. Bainite also contributed to high BH values, particularly in the 0 and 2 pct prestrain and aged conditions. Furthermore, differences in BH values amongst different TRIP steels were found to be composition dependent since composition controls the strain-induced transformation of retained austenite to martensite, which affects BH levels. Ramazani et al. [11] found that BH values continued to increase as a function of prestrain for a TRIP 700 steel up to a maximum of 5 pct prestrain before decreasing with additional prestrain. They attributed the prestrain dependence of strengthening to the amount of retained austenite that transforms to martensite, which is dependent on prestrain and austenite stability, and subsequent tempering of martensite during aging. Unlike DP steels, they did not observe overaging in the TRIP steel at higher temperature, longer time aging. Zhang et al. [13] investigated the effect of microstructure on the BH behavior of a CMnSi TRIP steel. Differences in strengthening and yielding behavior were attributed to differences in the amount of polygonal ferrite and the generation of dislocations and dislocation structures in this phase. Timokhana et al. [5,6] used TEM and APT to suggest that the BH behavior of TRIP steel is controlled by the formation of dislocation cell structures in ferrite and the high carbon content of ferrite. They also observed the transformation of retained austenite to martensite. Das et al. [14] found that the presence of bainite in TRIP steel can lead to considerable BH response due to the presence of many dislocations and high amount of carbon atoms, leading to dislocation pinning.

Through vehicle lightweighting efforts, sheet steels with tensile strengths exceeding 1 GPa have begun to see widespread use by OEMs. Therefore, it is essential that automotive engineers understand in-service material properties of these new higher-strength grades after part forming and paint baking operations. Limited research has been conducted on the BH behavior of sheet steels with as-received tensile strengths exceeding 1 GPa. This study aims to quantify the BH behavior of select AHSS grades as a function of time, temperature, and level of prestrain.

2. Materials and Experimental Procedure

2.1. Materials

Five sheet steels with ultimate tensile strengths exceeding 1 GPa were selected for this study. Materials investigated were press hardenable steels (PHS) 1500 and 2000; TRIP aided bainitic ferrite (TBF) 1000 and 1200; and dual phase (DP) 1000. Number designations refer to minimum as-received (AR) ultimate tensile strengths in MPa. DP and TBF steels were industrially produced and tested in the uncoated condition. PHS steels were produced using laboratory scale hot stamping lines. Blanks were austenitized at 930 °C with hold times of 6.5 min for PHS 1500 and 3.25 min for PHS 2000. PHS 1500 was initially Al-Si coated prior to heat treatment to prevent decarburizing. After hot stamping, the coating was mechanically removed via surface grinding. PHS 2000 was

uncoated and was austenitized in a controlled atmosphere then shot blasted after hot stamping to remove scale. Following austenitization, blanks were transferred to water-cooled flat dies that imposed no significant deformation and quenched to form fully martensitic microstructures. Sheet thicknesses were 1.00 mm (TBF 1000), 1.50 mm (DP 1000 and PHS 2000), and to 1.56 mm (TBF 1200 and PHS 1500). The chemical compositions of the experimental steels are given in Table 1. Elements not reported in chemical analyses are shown as N/R in the table.

2.2. Bake Hardening Simulation

The automotive paint baking cycle was simulated using a range of industrially relevant times and temperatures. Tensile testing was performed on DP and TBF specimens subjected to paint baking times ranging from 15 to 60 min, temperatures from 120 to 200 °C, and prestrains from 0 to 5 pct. Times, temperatures, and prestrains were chosen to reflect possible combinations of part forming strains and subsequent BIW paint baking times/temperatures observed in real-world automotive assembly plants. Tests were also performed for these steels in the AR condition. Table 2 shows all conditions tested for these grades.

Press hardening, also known as hot stamping or hot press forming, eliminates the potential of springback by forming parts in the austenite phase, due to low flow stress at high temperatures, then immediately quenching the parts inside the die [15,16]. Because no additional part forming occurs after austenite is quenched to martensite, PHS 1500 and PHS 2000 were not experimentally prestrained and thus bake hardening assessed the low temperature tempering (LTT) of martensite [17]. These two steels were heat treated using the time/temperature conditions that exclude prestrain listed in Table 2.

Thermal treatments for the five steels were performed in a hot oil bath using glycol-based heat transfer fluid. An oil bath was selected to ensure good thermal flux, reduced oxidation, and consistent temperature. Temperature was controlled within ±1 °C and was checked periodically using a thermometer with a precision of ±0.1 °C for the duration of the heat treatment. A timer was started when the samples were placed in the bath. When the timer expired, samples were immediately quenched in water. It is assumed that specimens immediately reached the baking temperature once placed in the bath. Therefore, the times in Table 2 represent the total time at temperature for a given condition. Times and temperatures listed in this table were used to obtain an equivalent tempering parameter, as will be discussed in Section 2.5.

TABLE 1 Chemical Composition of Selected Steel Grades

wt pct	C	Mn	Si	Ni	Cr	Ti	Al
PHS 1500	0.24	1.16	0.21	N/R	0.22	0.03	0.04
PHS 2000	0.34	1.27	0.23	0.06	0.14	70*	0.03
DP 1000	0.17	2.28	0.19	0.02	0.50	20*	0.05
TBF 1000	0.17	2.37	1.48	0.03	0.06	30*	0.05
TBF 1200	0.20	2.51	1.51	0.03	0.05	40*	0.05

wt pct	B*	Mo	Cu	Co	Nb	V*	W
PHS 1500	30	-	N/R	N/R	N/R	N/R	N/R
PHS 2000	16	0.02	0.01	0.02	0.04	80	0.01
DP 1000	3	0.01	0.02	40*	0.02	40	0.02
TBF 1000	3	0.01	0.02	40*	0.02	30	0.02
TBF 1200	3	0.08	0.02	30*	20*	40	0.02

* ppm

TABLE 2 Test Matrix for DP, TBF, and PHS (No Prestrain)

Temperature [°C]	Time [min]	Prestrain [pct]	T[K]* (11.8+logt[s])
AR	AR	AR	-
120	20	0	5850
120	20	2	5850
160	15	0	6391
160	15	2	6391
160	15	5	6391
160	60	0	6652
160	60	2	6652
160	60	5	6652
170	20	0	6594
170	20	2	6594
170	20	5	6594
200	15	0	6981
200	15	2	6981
200	15	5	6981
200	60	0	8266
200	60	2	7266
200	60	5	7266

2.3. Tensile Testing

All tensile samples were manufactured via wire electrical discharge machining (EDM) to produce ASTM E8 sheet-type standard size specimens [18]. Length of reduced parallel section and width were machined to 57.15 mm and 12.7 mm, respectively. Width and thickness were subsequently verified and recorded using a micrometer capable of 0.001 mm precision. Machining was done with the gauge length (tensile axis) parallel to the rolling direction. Uniaxial tensile testing followed ASTM E8 standards and was performed on a displacement controlled electromechanical load frame. A crosshead speed of 1.25 mm/min was chosen to generate an engineering strain rate of approximately 3.7×10^{-4} s^{-1}. A clip-on extensometer configured with a total gauge length of 50.8 mm was used to collect displacement data. The extensometer featured knife edge-type grips and double-sided tape was attached on the surface of the tensile bars to prevent the extensometer from slipping during testing. Three test replicates were performed for each condition listed in Table 2. Load data were measured with a load cell rated to 89 kN. Load-displacement data and gauge measurements were used to

calculate engineering stress and strain values. From these data, yield strength, (YS), upper and lower yield strength (UYS and LYS), ultimate tensile strength (UTS), uniform elongation (UE), and total elongation (TE) measurements were determined, along with the bake hardening response.

2.4. Assessment of Bake Hardening: BH_x and $\Delta\sigma$

The strengthening effect due to the paint baking operation is quantified using the BH index, BH_x, which is measured as the difference between the flow stress, σ_f, at the end of x pct prestrain and the lower yield stress, σ_a, after baking at a certain time and temperature [4,19,20]. For example, BH_0 is unstrained (no prestrain); BH_2 and BH_5 are prestrained 2 and 5 pct, respectively. Figure 1(a) schematically shows how BH_x is calculated for a material that has discontinuous yielding (*i.e.* a yield point drop). In the present work, braces (or curly brackets) are used to designate specific prestrain/temperature/time conditions using the following convention: {*x*-*y*-*z*}, where *x* is prestrain in pct, *y* is temperature in Celsius, and *z* is time in minutes. Engineering stress after paint baking was determined using the original cross-sectional area (*i.e.* measured prior to prestraining) to prevent a reduction in area after prestrain from inflating post-BH results. This has been shown to be substantial when prestrains exceed 5 pct and a significant decrease in cross-sectional area can be expected [11,12]. Furthermore, UE and TE elongation measurements exclude strain from prestraining. Strain is reported after baking only.

FIGURE 1 Measurement of BH and $\Delta\sigma$ response for TBF 1000 after 2 pct prestrain and baked at (a) 170 °C for 20 min and (b) 120 °C for 20 min. When yielding is discontinuous, as in (a), BH_x is approximately equal to $\Delta\sigma$. However, if yielding is continuous, shown in (b), and the 0.2 pct offset method is used to calculate YS, the steel will work harden from σ_f to σ_a and will be included in BH_x. This figure uses experimental data to illustrate the method proposed by Waterschoot et al. [4].

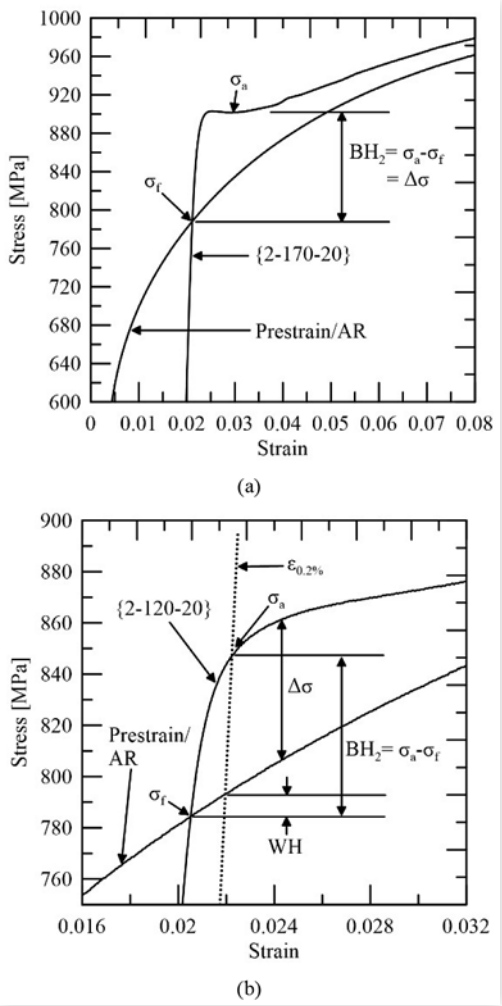

The absence of a yield point phenomenon after prestraining and baking makes determination of BH difficult. If no distinct yield point exists, the 0.2 pct offset yield strength (YS) method is used to determine σ_a according to ASTM E8. Figure 1(b) shows how BH_x is calculated in the absence of a marked yield point. Figure 1(b) also shows, however, that valuable information about the BH behavior may be lost using this method because a high rate of work hardening (WH) contributes a significant portion to BH [4,10]. For this reason, Waterschoot et al. [4] have suggested using an alternative approach: a flow curve after prestraining and baking is superimposed on an unaged flow curve. The difference between these two curves (*i.e.* prestrained and baked curve minus unaged curve) results in a $\Delta\sigma$ curve as a function of strain. The maximum of the $\Delta\sigma$ curve, hereafter referred to as $\Delta\sigma_{max}$, is taken as a measure of the increase in YS due to strain aging only. As an example, $\Delta\sigma$ is equal to BH if a clear yield point is observed, as shown on Figure 1(a). Both methods, BH_x and $\Delta\sigma$, were used to analyze data and results are presented in the next section.

2.5. Tempering Parameter

A widespread method to assess martensite tempering and the effect of both time and temperature on mechanical properties is to combine time and temperature into a single variable known as a tempering parameter. In 1945, Hollomon and Jaffe [21] were able to construct a method for calculating, for any steel, the temperature necessary to temper to a desired hardness for a selected time or, conversely, the time necessary to temper to a desired hardness at a selected temperature. Understanding that tempering is a diffusion-related process, they derived Equation (1) from an Arrhenius-type equation:

$$H = f\left(T\left(c + \log t\right)\right) \tag{1}$$

where H is hardness, T is temperature in Kelvin, c is a constant, and t is time in seconds. It was found that the constant c is moderately dependent on steel grade, and that a value of c between 10 and 16 introduces a hardness error on the order of one-point Rockwell C. In this study, a value of 11.8 was chosen. The multiplying effect of temperature and the log of time reflects the greater importance of temperature on producing diffusion-dependent microstructural changes [22]. One limitation of Equation (1) is with alloyed steels: tempering alloyed steels at higher temperatures may lead to secondary hardening which is not accounted for by this equation [17,22].

2.6. Stress-Strain Analysis

Deformation behavior is commonly modeled with an idealized mathematical stress-strain equation to simplify discussion of strain hardening. The most recognized stress-strain equation is the Hollomon equation [23]:

$$\sigma = K\varepsilon_{plastic}^{n} \tag{2}$$

where σ is true stress, K is the strength coefficient, $\varepsilon_{plastic}$ is plastic true strain, and n is the strain-hardening exponent. Equation (2) models the flow curve in the region of uniform plastic strain by a simple power curve relation. Deviations from the Hollomon equation are often observed for "non-ideal" materials. Several equations have been derived to model such deviations and amplify distinct regions of strain hardening, with a common variation being given by Ludwik [24]:

$$\sigma = \sigma_0 + B\varepsilon_{plastic}^{m} \tag{3}$$

where σ is true stress, σ_0 is the yield stress, B and m are empirical parameters, and $\varepsilon_{plastic}$ is the plastic component of true total strain. Following Equation (3), the stages of strain hardening can be delineated by differentiating and rewriting, using logarithm rules, such that:

$$log\left(\frac{d\sigma}{d\varepsilon}\right) = log\left(Bm\right) + \left(m-1\right)\cdot log\left(\varepsilon_{plastic}\right) \tag{4}$$

A *Jaoul-Crussard* plot [25] is a log-log plot of strain hardening rate as a function of true plastic strain. According to Equation (4), a material that follows the Ludwik equation will yield a straight line with slope $(m - 1)$. This procedure is particularly sensitive to variations in strain hardening rate at low strains. For example, when stress-strain curves transition from continuous to discontinuous, the trend will no longer be linear. In the results considered below, application of Equation (4) was used to explicitly show changes in yielding behavior for LTT PHS grades.

3. Results

Tensile testing was completed using the experimental procedures outlined in subsections 2.2 and 2.3. Results are presented below for the five grades and are organized based on strength as follows: DP 1000, TBF 1000, TBF 1200, PHS 1500, and PHS 2000.

3.1. As-Received (AR) Tensile Properties

All steel grades were tested in the AR condition. Figure 2 shows representative engineering stress-strain curves and Table 3 summarizes average YS, UTS, UE, and TE for each experimental material. As previously mentioned, material number designation refers to AR UTS. The DP and TBF grades were each within 15 MPa of each respective designation. DP 1000 and TBF 1000 had similar UTS despite significantly different YS, reflecting differences in strain hardening. The press hardened grades, however, exceeded strength designation by 92 MPa (PHS 1500) and 112 MPa (PHS 2000). Despite the large difference in UTS, PHS 1500 and PHS 2000 had similar TE. Figure 2 shows that the materials selected for this study have significantly different yielding behaviors, strengths, and ductilities.

FIGURE 2 Engineering stress-strain curves for as-received DP 1000, TBF 1000, TBF 1200, PHS 1500, and PHS 2000.

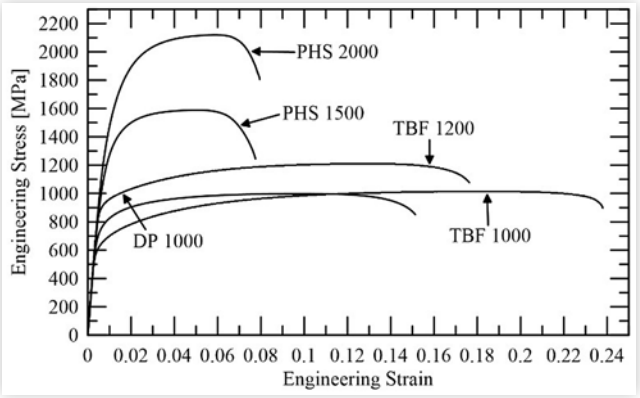

TABLE 3 As-Received Tensile Properties of All Steel Grades

Steel Grade	YS [MPa]	UTS [MPa]	UE [pct]	TE [pct]
DP 1000	736	998	9.9	15.4
TBF 1000	623	1015	18.2	23.3
TBF 1200	905	1212	13.0	17.7
PHS 1500	1184	1592	4.9	7.9
PHS 2000	1432	2115	5.7	7.9

3.2. Results for DP1000

Load-displacement data for DP 1000 were collected and then converted to engineering stress-strain data. Figure 3 shows engineering stress-strain curves obtained for AR and select samples prestrained 0, 2, and 5 pct followed by baking. Figures 4(a)-(c) show tensile properties for these tests and all others plotted as a function of tempering parameter. Considering first the 0 pct prestrain condition, Figure 3 shows that the highest and longest time/temperature (200 °C, 60 min) led to discontinuous yielding followed by a reduction in strain hardening rate compared to AR. Recorded YS for {0-200-60} was 849 MPa, which gave corresponding BH_0 and $\Delta\sigma_{max}$ values of 117 and 165 MPa, respectively. Other samples tested in the unstrained and baked condition did not show discontinuous yielding, but did, however, show an appreciable increase in YS. Figure 4(a) shows tensile properties of unstrained and baked DP 1000 plotted as a function of tempering parameter. Yield strength continuously increases as baking time/temperature (*i.e.* tempering parameter) increases. On the other hand, ultimate tensile strength remains relatively unchanged. Because these two curves converge (or alternatively the YS/UTS ratio increases) at larger tempering parameters, it can

FIGURE 3 Engineering stress-strain curves for DP 1000 tested in the following conditions: AR; unstrained and baked 200 °C, 60 min; prestrained 2 pct and baked 160 °C, 60 min; and prestrained 5 pct and baked 170 °C, 20 min.

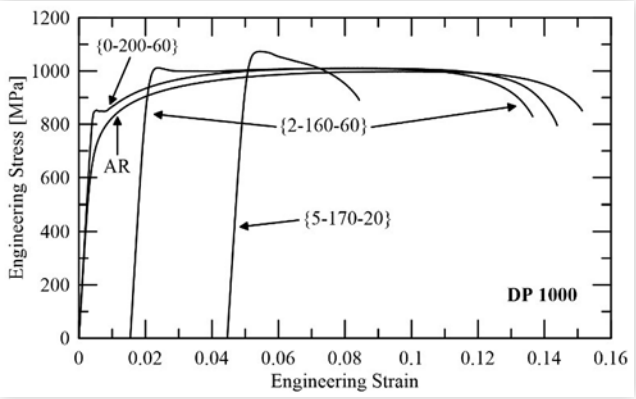

be rationalized that the strain hardening rate decreased with increasing aging. Despite large increases in YS for these samples, Figure 4(a) shows that tensile ductility was relatively unaffected. The greatest decrease in UE and TE, from the lowest to the highest tempering parameter, was 9.5 to 8.3 pct and 15.2 to 14.1 pct, respectively.

Introducing prestrain prior to paint baking for DP 1000 significantly increased strength and produced yield point phenomena. Referring again to Figure 3, an engineering stress-strain curve was plotted for {2-160-60}. All prestrain curves hereafter were omitted from figures for all steels and conditions. LYS for this condition increased to 1003 MPa resulting in a BH_2 of 91 MPa and a $\Delta\sigma_{max}$ of 99 MPa. Accounting for the other conditions not shown on this plot, the smallest increase in strength (with respect to BH_2 and $\Delta\sigma_{max}$) was observed for the {2-120-20} condition and was approximately 45 MPa for both properties. Conversely, the greatest increase was for {2-200-60} resulting in a BH_2 of 108 MPa and $\Delta\sigma_{max}$ of 130 MPa. Plotting tensile properties as a function of tempering parameter, Figure 4(b) shows that the YS/UTS ratio significantly increases, especially at larger tempering parameters, compared to the unstrained conditions. Ultimate tensile strength increases with increasing tempering parameter but is matched by equally increasing LYS. Consequently, strain hardening diminished for the 2 pct prestrain conditions. Figure 4(b) also shows that UE and TE decrease substantially with increased aging. For example, relative to AR, UE of {2-200-60} decreased by over 50 pct from 9.9 pct (AR) to under 4.7 pct.

Increasing prestrain to 5 pct again led to increased strength gains after baking compared to the unstrained conditions. Figure 3 shows a large increase in YS compared to AR for {5-170-20}. Recorded YS was 1053 MPa which produces a BH_5 of 69 MPa and $\Delta\sigma_{max}$ of 92 MPa. YS values for this prestrain level at all baking conditions were determined using the 0.2 pct offset strain method because no yield point phenomena were observed. Samples appeared to yield and then transition directly to post-uniform instability until failure with very limited ductility due to significantly reduced strain hardening. Figure 4(c) reflects this behavior because

FIGURE 4 Tensile properties of DP 1000 prestrained 0 (a), 2 (b), and 5 pct (c) plotted as a function of tempering parameter.

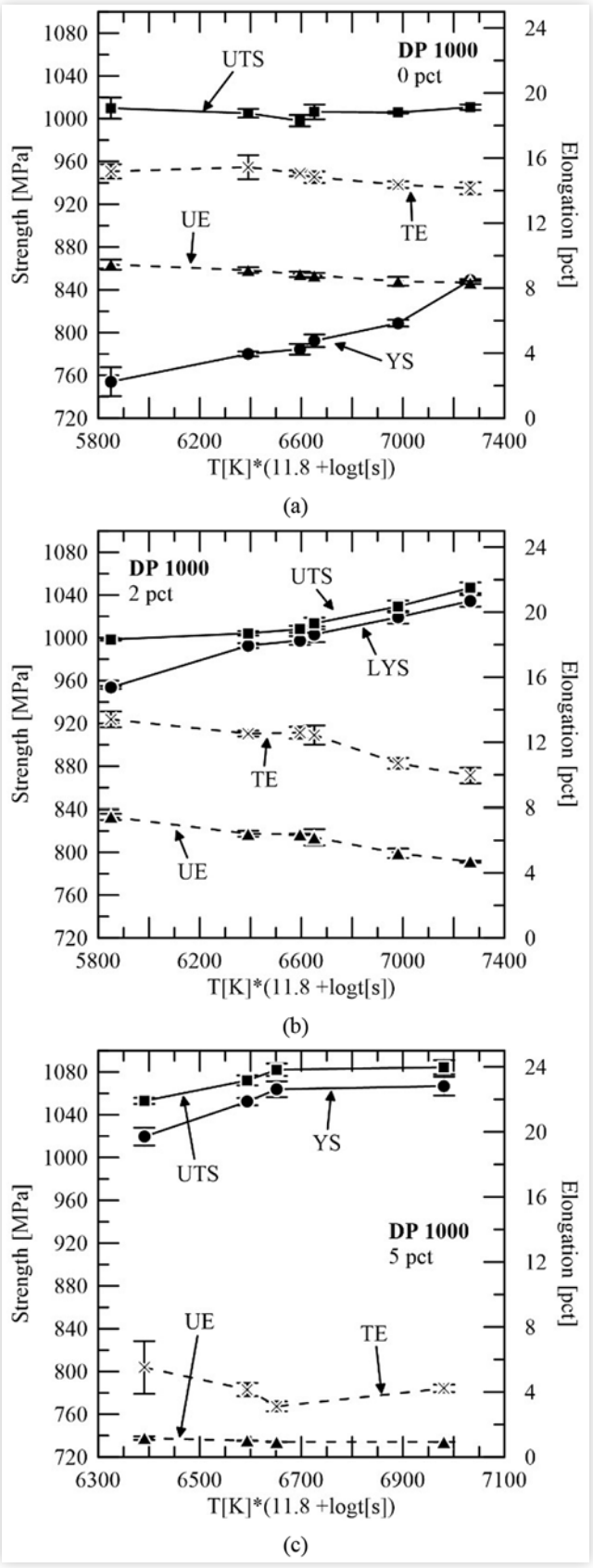

FIGURE 5 Engineering stress-strain curves for TBF 1000 tested in the following conditions: AR; unstrained and baked 200 °C, 60 min; prestrained 2 pct and baked 200 °C, 60 min; and prestrained 5 pct and baked 160 °C, 60 min.

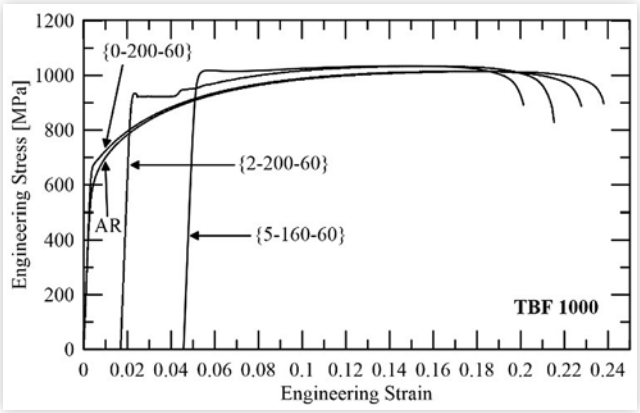

UTS and YS curves are closely spaced and nearly parallel. This figure also shows the substantial decrease in ductility (UE and TE) for samples prestrained 5 pct. Uniform elongation after baking was approximately 1 pct for all samples. This decrease in ductility also manifested itself in the {5-200-60} tests because all samples failed at the fillet of the tensile specimen and outside the extensometer. Therefore, this condition was omitted from Figure 4(c).

3.3. Results for TBF1000

In a similar fashion to DP 1000, TBF 1000 was tensile tested using the test matrix in Table 2. Figure 5 presents select engineering stress-strain curves prestrained 0, 2, and 5 pct and baked at various times and temperatures. Figures 6(a)-(c) plot YS, UTS, UE, and TE as a function of tempering parameter for all test conditions. Beginning with the unstrained and baked test, Figure 5 shows the stress-strain curve for {0-200-60} which exhibits continuous yielding. This condition had the greatest increase in YS out of all unstrained conditions; recorded BH_0 and $\Delta\sigma_{max}$ values were 60 MPa and 81 MPa, respectively. All other unstrained tests at various baking times/temperatures also showed continuous yielding and increases in YS. Figure 6(a) illustrates the relationship between YS, UTS, UE, and TE as a function of tempering parameter for BH_0 tests. As tempering parameter increases, YS increases and UTS remains relatively unchanged. Like the DP steel, this indicates decreased strain hardening as paint baking time and temperature increased. Figure 6(a) also shows that ductility is almost unaffected in the absence of prestrain. The largest decrease was for the {0-200-60} condition and was less than 1 pct for both UE and TE relative to AR.

With the addition of 2 pct prestrain, TBF 1000 displayed a marked increase in YS (measured as LYS for instances of discontinuous yielding) compared to the AR condition, as observed in Figure 5 for the representative {2-200-60} test. The samples prestrained 2 pct had long, pronounced YPE and LYS ranging from 850 ({2-120-20}) to 920 MPa ({2-200-60}). Maximum BH_2 and $\Delta\sigma_{max}$ values of 120 and 130 MPa,

FIGURE 6 Tensile properties of TBF 1000 prestrained 0 (a), 2 (b), and 5 pct (c) plotted as a function of tempering parameter.

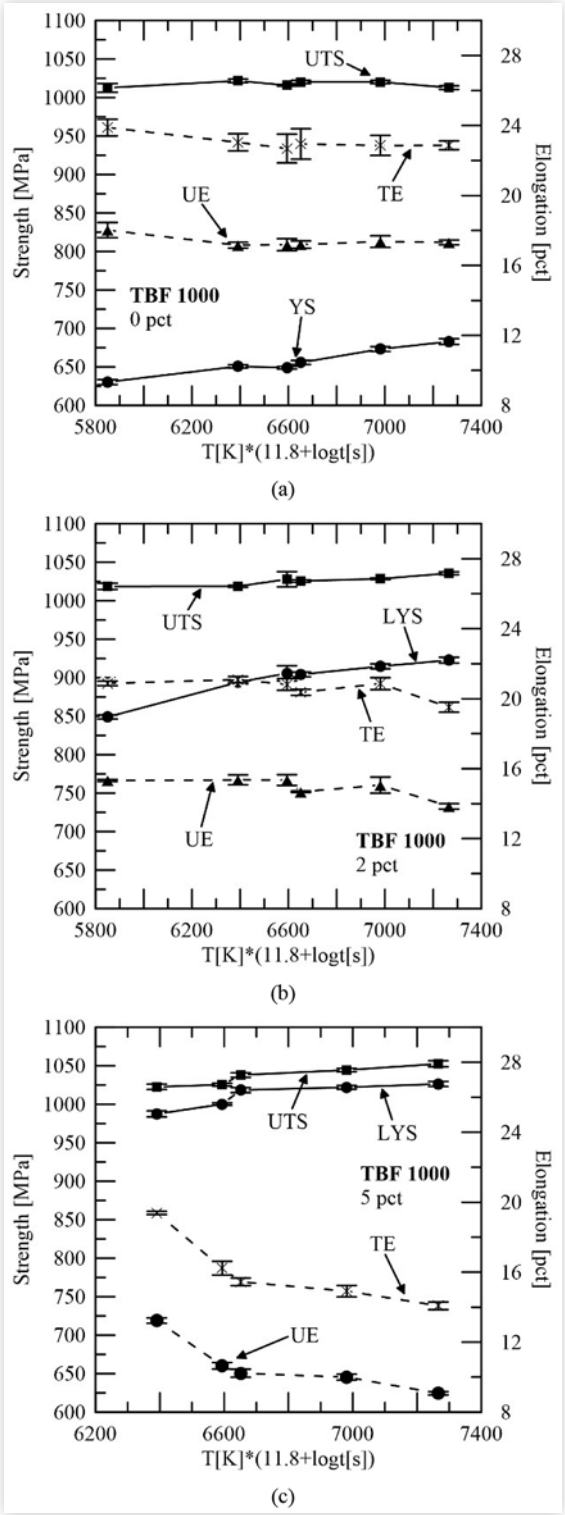

respectively, were recorded after baking at 200 °C for 60 min. Figure 6(b) shows this increasing trend in LYS as a function of tempering parameter. The figure also shows that UTS only slightly increases. Again, the convergence of the LYS and UTS curves suggests decreased strain hardening rate as baking

time and temperature increased. With respect to ductility, as seen in Figure 5(b), UE and TE slightly decreased to a minimum at the highest tempering parameter.

When prestrain was increased from 2 to 5 pct, LYS increased substantially to over 1000 MPa for all conditions except {5-160-15}, which had a LYS of approximately 990 MPa. An engineering stress-strain curve for {5-160-60} is presented in Figure 5 which shows the general yielding behavior for 5 pct prestrained samples. This sample discontinuously yields followed by a substantial period of limited strain hardening before failure. Figure 6(c) shows tensile properties for 5 pct prestrained samples. The closely spaced, nearly parallel, and slightly increasing LYS and UTS curves indicate low strain hardening that was insensitive to baking time/temperature. In other words, strain hardening did not change with increasing time/temperature. Conversely, tensile elongation continuously decreased with increasing tempering parameter with values decreasing from 13 to 9 pct for UE and 19 to 14 pct for TE.

3.4. Results for TBF1200

The third and final prestrained steel is TBF 1200. Stress-strain data from select tensile tests are plotted in Figure 7. Figures 8(a)-(c) show tensile properties for 0, 2, and 5 pct prestrain plotted as a function of tempering parameter for all tests. Beginning with 0 pct prestrain conditions, Figure 7 presents an engineering stress-strain curve for {0-200-60}. This figure shows that, like DP 1000 and TBF 1000, baking in the absence of prestrain can create a considerable increase in YS and flow stress at low strains. Referring to other tests not shown on this plot, for all conditions except {0-120-20}, heat treating led to sizeable increases in YS. The largest increase was observed for the {0-200-60} and was recorded for BH_0 and $\Delta\sigma_{max}$ to be 81 and 98 MPa, respectively. Figure 8(a) shows that UTS does not change substantially with increasing baking time/temperature. However, YS increases continuously. Like the two

FIGURE 7 Engineering stress-strain curves for TBF 1200 tested in the following conditions: AR; unstrained and baked 200 °C, 60 min; prestrained 2 pct and baked 160 °C, 60 min; and prestrained 5 pct and baked 200 °C, 60 min.

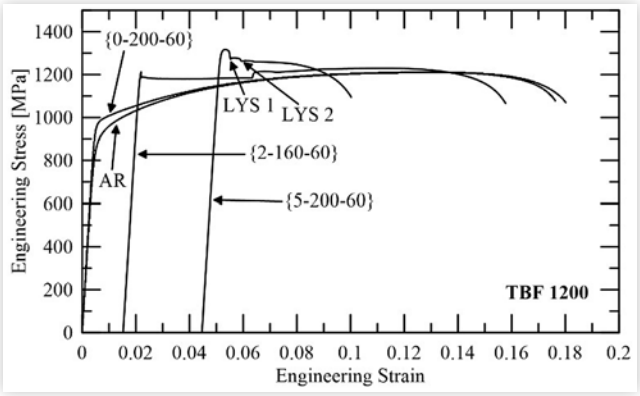

FIGURE 8 Tensile properties of TBF 1200 prestrained 0 (a), 2 (b), and 5 pct (c) plotted as a function of tempering parameter.

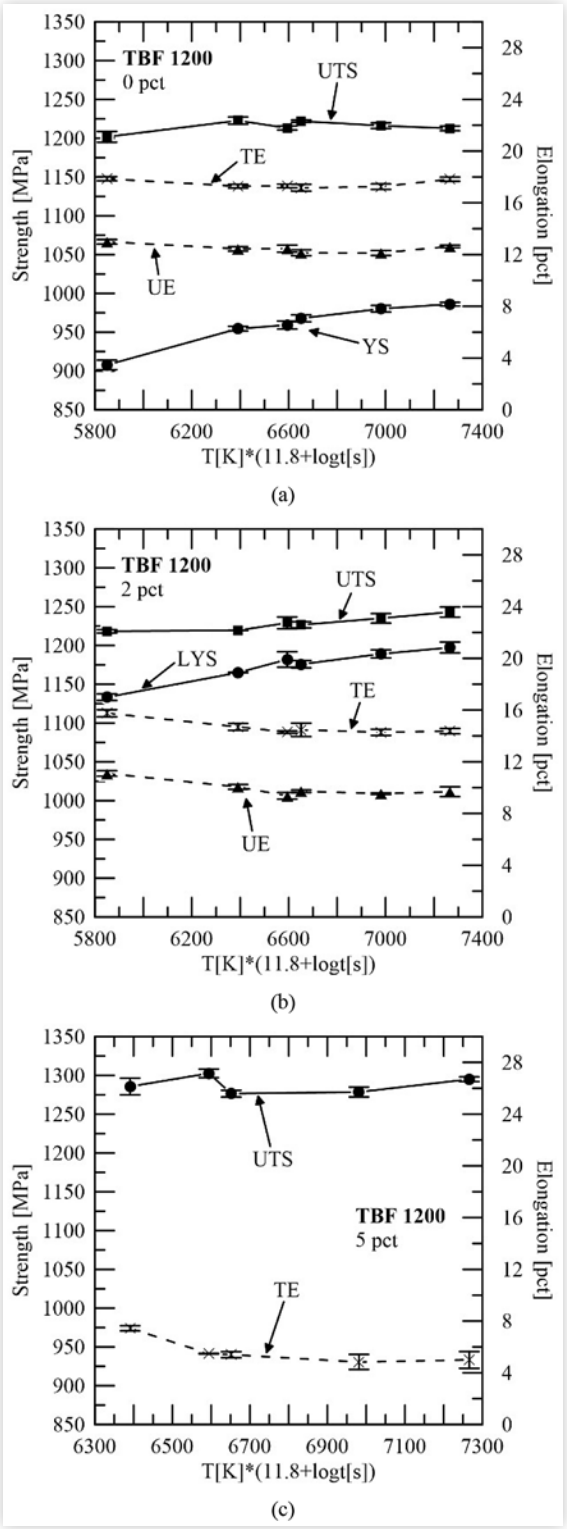

previous steels, YS and UTS curves for the unstrained and baked conditions converge indicating a reduction in strain hardening as tempering parameter increases. Figure 8(a) also shows that tensile elongations are similar amongst all tests with the max difference between baked tests being approximately 0.8 pct, which was measured for the {0-160-60} condition.

Adding 2 pct prestrain prior to baking changes the yielding behavior of TBF 1200 from continuous to discontinuous, as shown by the representative engineering stress-strain curve for {2-160-60} in Figure 7. Unlike the unstrained conditions, adding prestrain led to discontinuous yielding with large YPEs (between 3 and 5 pct depending on baking condition), even at the shortest time and lowest temperature of 120 °C, 20 min. Figure 7 shows that YPE is followed by a small increase in stress, and a period of very low strain hardening until failure. Figure 8(b) plots LYS and UTS as a function of tempering parameter. At the lowest time/temperature, an appreciable difference between the LYS and UTS is observed. As tempering parameter is increased, this difference decreases as the rate of change in LYS with tempering parameter is higher than observed for UTS values. The convergence in LYS and UTS values reflects decreasing strain hardening as time/temperature increases. Tensile elongations are also plotted in Figure 8(b). UE and TE do not change significantly with increasing time/temperature - less than 1.5 pct for both. Compared to the AR condition, however, UE decreased by 3.3 pct and TE decreased by 3.4 pct relative to the longest time, highest temperature paint baking condition {2-200-60}.

Considering 5 pct prestrain, higher time/temperature samples showed unique yielding behavior. Figure 7 displays an engineering stress-strain curve for {5-200-60}. As labeled on the figure, this sample showed two drops in the stress-strain curve labeled "LYS 1" and "LYS 2". Succeeding the UYS, there is a drop in stress associated with "LYS 1". This drop is then followed by a short interval of slightly decreasing stress which is perhaps associated with YPE. This period is followed by another drop in stress, "LYS 2", then decreasing flow stress to failure. This behavior was not unique to {2-200-60} but was also observed for {2-160-60} and {2-200-15}. Figure 8(c) plots UTS and TE for TBF 1200 after 5 pct prestrain and baking. LYS and UE have been omitted because no clear LYS or UE was identified. Samples yielded then proceeded to post-uniform instability without significant work hardening. Instead, UTS, which is presumably identical to UYS, and TE have been plotted. UTS is observed to randomly fluctuate between 1275 and 1300 MPa. TE decreases gradually as tempering parameter increases. Relative to AR, TE decreased substantially from 17.7 pct (AR) to 5.0 pct ({5-200-60}).

3.5. Results for PHS 1500

Figure 9 shows PHS 1500 engineering stress-strain curves obtained for AR and for specimens tempered at 170 °C for 20 min and 200 °C for 60 min. PHS 1500 was not prestrained due to the nature of the hot stamping process. The ultimate tensile strength of the AR material was approximately 1590 MPa. Tempering at 170 °C for 20 min and 200 °C for 60 min decreased the UTS to 1570 MPa and 1530 MPa, respectively. Total elongation of the {0-170-20} specimen (7.6 pct)

FIGURE 9 Engineering stress-strain curves for PHS 1500 in the AR and condition and tempered at 170 °C for 20 min and 200 °C for 60 min.

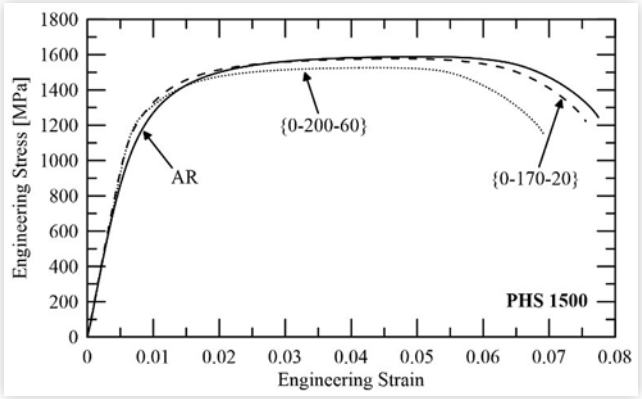

nearly matches that of the AR (7.7 pct), but the TE of {0-200-60} decreased slightly (7.3 pct). All conditions exhibited continuous yielding, but after tempering a transition in yielding behavior was observed. Increasing proportionality limits followed by decreasing strain hardening rates, as a function of increasing tempering, indicate incipient discontinuous yielding. At some increased tempering intensity, it is expected that the material will fully transition and exhibit discontinuous yielding. The highest stress at which stress is directly proportional to strain is noticeably lower for the AR material than for either LTT conditions. Likewise, the yield strength measured using the 0.2 pct offset method was approximately 1190 MPa for AR and increased to 1270 MPa and 1275 MPa for {0-170-20} and {0-200-60}, respectively.

The continuous decrease in UTS reflects the decreasing ability of the specimens to strain harden as tempering intensity increases. Figure 10 presents a log-log plot of strain hardening rate as a function of true plastic strain, following Equation (4), for PHS 1500. The AR specimen shows nearly linear behavior throughout the entire range of plastic strains, indicating good agreement with the Ludwik equation (Equation (3)). After tempering at 170 °C for 20 min, however,

FIGURE 10 Log-log plot of strain hardening rate as a function of true plastic strain for PHS 1500 in the AR and tempered conditions.

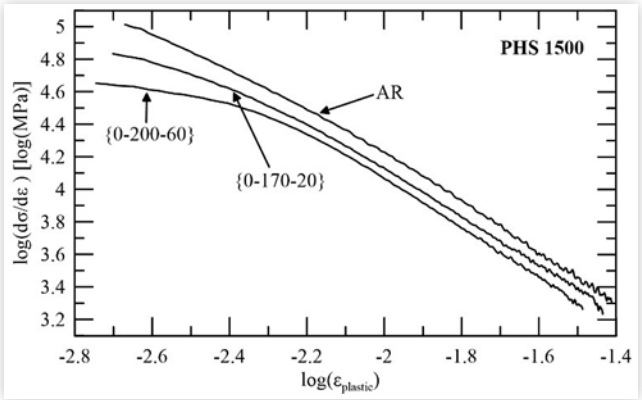

strain hardening rate significantly decreased (note the logarithm axes) at low plastic strains and to a lesser extent at higher plastic strains. This behavior is amplified for the higher temperature, longer time temper. Moreover, at low strains, the change from linear behavior of the AR to progressively more curved behaviors for increasing tempering intensities clearly indicates a change in yielding behavior. The AR has a gradual transition from elastic to plastic with initially high strain hardening and follows a power curve. The tempered materials, however, have an abrupt yielding phenomenon indicated by the low strain hardening rate at low strain, as observed in Figure 9.

3.6. Results for PHS 2000

Figure 11 presents representative engineering stress-strain curves for PHS 2000 in the AR condition and tempered at 170 °C for 20 min and 200 °C for 60 min. This hot stamped steel was not prestrained. The UTS of AR PHS 2000 was determined to be 2120 MPa. Tempering decreased UTS values to 2000 MPa and 1850 MPa after tempering at 170 °C for 20 min and 200 °C for 60 min, respectively. Total elongations did not significantly differ between AR and LTT conditions and were approximately 8 pct; ductility did not appear to benefit from LTT. Like PHS 1500, PHS 2000 shows signs of changes from continuous to discontinuous yielding. The proportionality limit for the AR appears to be lower than both tempering conditions as indicated by Figure 11. Yield strengths determined with the 0.2 pct offset method, were found to be 1430 MPa for AR; 1600 MPa for {0 pct, 170 °C, 20 min}; and 1562 MPa for {0 pct, 200 °C, 60 min}.

As with PHS 1500, the continuous decrease in tensile strength of PHS 2000 reflects the decreasing ability of the specimens to strain harden as tempering intensity increases. Figure 12 presents a Jaoul-Crussard plot of strain hardening rate as a function of true plastic strain for PHS 2000. The AR specimen did not behave perfectly linear like PHS 1500, slightly deviating from the Ludwik equation. Both tempering conditions, though, decreased strain hardening rate at all strain levels, but with a more pronounced effect at lower strain levels (recall the logarithmic axes). Furthermore, there is a decrease in the radius of curvature (*i.e.* increase in bending of curves), at low strains, with increasing tempering intensities. At high strains, the curves become nearly parallel. The increase in curvature at low plastic strains is an indication of changing yielding behavior with increasing tempering. Figure 11 reflects this observation; the most severe tempering ({0 pct, 200 °C, 60 min}) has an initially high strain hardening rate at yielding followed by a highly strain-dependent decrease in strain hardening that does not follow a power curve relationship. On the other hand, the AR specimen yields gradually and more closely follows a power curve relationship.

FIGURE 11 Engineering stress-strain curves for PHS 2000 in the AR condition and tempered at 170 °C for 20 min and 200 °C for 60 min.

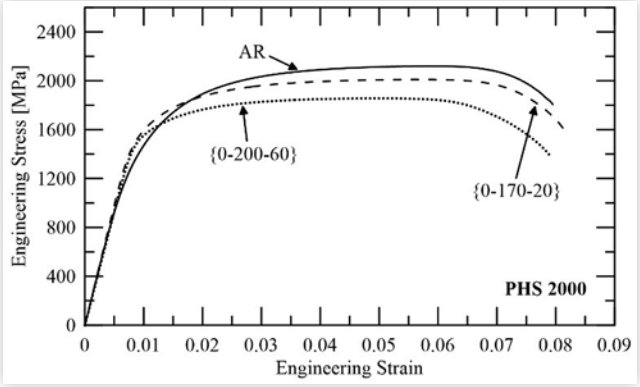

FIGURE 12 Log-log plot of strain hardening rate plotted as a function of true plastic strain for PHS 2000 in the AR and tempered conditions.

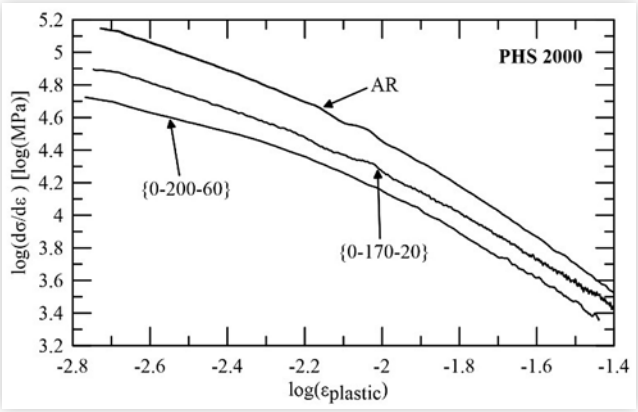

3.7. BH_0 Comparison for PHS Grades

Increases in YS, measured by BH_0, for the two PHS grades varied as a function of baking time and temperature as observed in the previous subsections. Figure 13 plots this variation in BH_0 as a function of tempering parameter for PHS 1500 and PHS 2000. Curves have been superimposed on both data sets to emphasize strengthening behavior. Starting from the lowest tempering parameter, BH_0 values for both grades appear to increase rapidly to a maximum as tempering parameter increases, then decrease. At the lowest tempering time and temperature ({0-120-20}), BH_0 for PHS 1500 and PHS 2000 were found to be approximately 23 MPa and 80 MPa, respectively. At the maximum, BH_0 reached 122 MPa for PHS 1500 and 175 MPa for PHS 2000. The maximum is followed by a decrease in BH_0. At any given time/temperature combination, PHS 2000 always has a larger strengthening response compared to PHS 1500. Despite the difference in strengthening, both curves appear to take the same shape with maxima at nearly the same tempering parameter.

3.8. BH vs $\Delta\sigma_{max}$

As shown in Section 2.4, $\Delta\sigma_{max}$ was suggested as an alternate parameter to assess bake hardening response for steels that exhibit continuous yielding after baking [4]. Use of $\Delta\sigma_{max}$

FIGURE 13 Strengthening response of unstrained and heat treated PHS 1500 and PHS 2000 as a function of tempering parameter. Curves have been drawn over the data sets to highlight trends in strengthening.

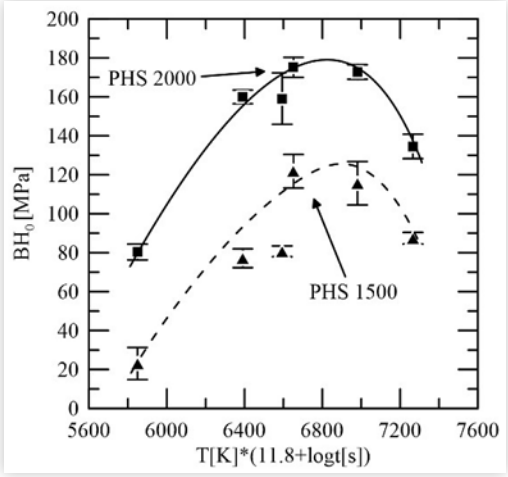

prevents measurements of bake hardening from being inflated by work hardening. Therefore, $\Delta\sigma_{max}$ should be less than BH_x for all tests that have continuous yielding. Conversely, if the steel exhibits discontinuous yielding, then both measures should be equal. It was of interest, then, to qualitatively compare $\Delta\sigma_{max}$ and BH_x for each steel to determine if this holds true. Figures 14(a)-(c) show BH_x plotted against $\Delta\sigma_{max}$ for DP 1000, TBF 1000, and TBF 1200 for all prestrain, time, and temperature conditions. For each grade/plot, a dashed line was drawn with a slope of one to indicate where BH_x is equal to $\Delta\sigma_{max}$. The magnitudes of the BH_x and $\Delta\sigma_{max}$ axes are equal to make this comparison possible.

Starting with DP 1000, Figure 14(a) shows BH_x plotted against $\Delta\sigma_{max}$ with the dashed line indicating equality. At low strengthening values, below 60 MPa, the two measures appear to be nearly identical. When strengthening increases, however, most of the points fall below the line indicating $\Delta\sigma_{max}$ is greater than BH_x. Similar behavior is observed for TBF 1200 in Figure 14(c) except for a noticeable grouping of data. Data grouped at lower strengthening values (between 60 and 100 MPa) belong to 0 pct prestrain conditions, while higher values (above 140 MPa) are shared between 2 and 5 pct. Nevertheless, data appear to be randomly ordered regardless if YPE or continuous yielding is present. On the other hand, TBF 1000 (Figure 14(b)) has many points on or near the line which suggests better agreement between BH_x and $\Delta\sigma_{max}$.

FIGURE 14 BH_x plotted against $\Delta\sigma_{max}$ for (a) DP 1000, (b) TBF 1000, and (c) TBF 1200 for all time, temperature, and prestrain combinations. A dashed line was added to each plot which represents where both measures are equal.

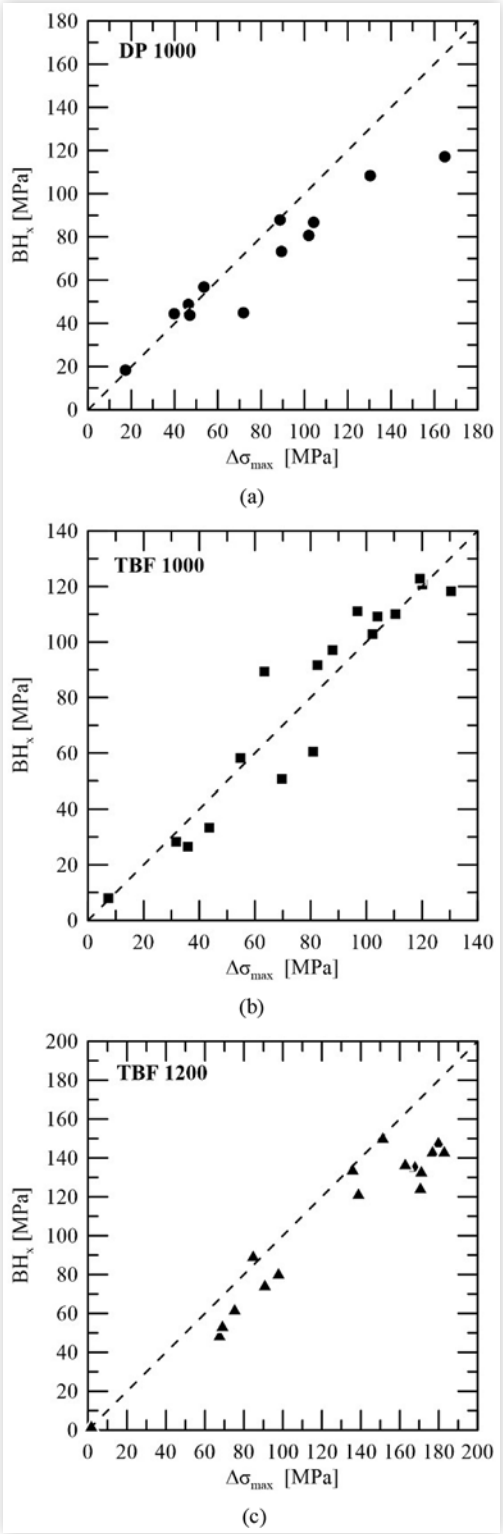

4. Discussion

4.1. BH_0 Results for DP, TBF, and PHS

All grades were subjected to simulated paint bake thermal histories and tensile tested without prestrain to determine tensile properties. Beginning with the DP and TBF grades, each steel

showed a constant increase in YS with increasing tempering parameter. At the lowest time/temperature, {0-120-20}, almost no changes in YS values were recorded. Conversely, the most significant increases, for these three grades, were documented for {0-200-60}. For example, the greatest increase in YS was for DP 1000 with corresponding BH_0 and $\Delta\sigma_{max}$ of 117 MPa and 165 MPa, respectively. Yielding remained continuous for these steels as time and temperature increased except for DP 1000 paint baked at 200 °C for 60 min. Increases in YS across these grades may be attributed to the immobilization of dislocations by free carbon in solution, which is supported by the return of the yield point phenomenon for DP 1000. Likewise, increasing YS with increasing time/temperature may be related to the time/temperature dependence of carbon diffusion proposed by Cottrell and Bilby [2]. It is interesting to note, however, that despite increases in YS, UTS for these grades did not change substantially indicating a decrease in strain hardening. Tensile ductility, either UE or TE, was relatively unaffected by baking. For each grade, maximum decreases in UE and TE relative to AR were less than one percent.

The martensitic PHS grades, on the other hand, exhibited different strengthening characteristics compared to the DP and TBF steels. Even at the lowest time/temperature ({0-120-20}), PHS 1500 and PHS 2000 had large increases in YS. Respective BH_0 were measured to be 23 and 80 MPa. Strengthening rapidly increased with increased time and temperature. For example, increasing temperature to 170 °C and holding for 20 min increased BH_0 to 81 MPa for PHS 1500 and 159 MPa for PHS 2000. Increases in YS by both steels may be a result of relaxation of internal stresses, formation of transition carbides, and/or pinning of dislocations [4,26]. Similar behavior has been documented for SAE 4300-series steels [27]. Differences in strength, shown in Figure 13, between the two steel grades are an outcome of different alloying. Table 1 shows that PHS 2000 has approximately 0.1 wt pct more carbon than PHS 1500. Dislocation density and transition carbide density increase with increasing carbon content accounting for the difference in strength of the steel [17,22]. Both PHS steels showed maxima on the BH_0 plot (Figure 13). The decrease in BH_0 at longer times, higher temperatures may be due to coarsening of transition carbides as tempering proceeds.

The transition from continuous to discontinuous yielding in the PHS steels was investigated with the aid of Jaoul-Crussard plots (Figures 10 and 12). The high densities of dislocations and transition carbides formed during autotempering and/or room temperature aging are responsible for the continuous yielding and high strain hardening rates for AR conditions [17,22]. Subsequent aging, however, decreased strain hardening which ultimately led to decreases in UTS. The specimens tempered at 200 °C for 60 min had the lowest tensile strengths. During tempering, it is likely that transition carbides coarsened, and dislocation densities decreased due to recovery mechanisms, both increasing the average free length of dislocations. According to the work hardening theory [28], an increase in free dislocation length will decrease flow stress and, correspondingly, strain hardening. Changes in yielding behavior and strain hardening were also seen in the baked DP and TBF steels and may be a result of similar effects.

4.2. BH_2 and BH_5 Results for DP and TBF

With the addition of prestrain, DP and TBF grades had yield strengths greater than paint baking alone, and YPE was observed for most steels and prestrain/time/temperature combinations. Generally, YS increased as tempering parameter increased for both 2 and 5 pct prestrained tests. The largest yield strengths were recorded at the highest temperature, longest time baking: 200 °C, 60 min. UTS did not significantly increase with increasing tempering parameter which is attributed to the decrease in strain hardening after prestrain and baking. Strain hardening is dependent on dislocation-dislocation interactions and dislocation interactions with barriers such as precipitates [29]. A high rate of strain hardening suggests obstruction of dislocations from gliding or cross-slipping on intersecting slip systems. A low rate of strain hardening, therefore, implies that a significant number of dislocations are either sessile or do not interact. Because the studied steels are known to have significant AR dislocation densities including those generated from prestraining, the low strain hardening rate may be attributed to effective pinning of dislocations by solute carbon. Other factors influencing strain hardening may be formation of dislocation cell structures during prestraining, transformation of retained austenite to martensite during prestraining, and/or coarsening of carbides [4, 5, 6, 7, 8, 9, 10, 11, 12, 13, 14].

Ductility for DP and TBF grades decreased as a function of prestrain and time/temperature. As tempering parameter increased, UE and TE generally decreased. The lowest UE and TE were recorded at 200 °C, 60 min. For example, after 2 pct prestrain and paint baking at this time/temperature, the UE of DP 1000 decreased relative to AR from 9.9 pct for AR to under 6.7 pct (including 2 pct strain from prestraining) for {2-200-60}. Decreases in UE and TE were also observed for TBF 1000 and TBF 1200 with the lowest ductility also recorded at 200 °C, 60 min. With respect to prestrain, tensile elongation was always lowest for 5 pct prestrain. Similar behavior has been reported by other authors and has been reported as the second stage of aging [8,10].

4.3. BH Comparison Between DP and TBF Grades

The Holloman-Jaffe tempering parameter was used to combine time and temperature into a single variable. Figures 15(a)-(c) show BH_x plotted as a function of tempering parameter for the three prestrain conditions: 0, 2, and 5 pct. Beginning with Figure 15(a), BH is plotted for 0 pct prestrain. The three steels (DP 1000, TBF 1000, and TBF 1200) show a steady increase in strengthening for nearly all tempering parameters. TBF 1000 had the least strengthening for nearly all tempering parameters ranging from approximately 0 MPa up to 60 MPa at the most severe paint baking time/temperature. On the other hand, both

FIGURE 15 BH_x plotted as a function of tempering parameter for (a) 0 pct prestrain, (b) 2 pct prestrain, and (c) 5 pct prestrain. Regardless of prestrain amount, strengthening appears to almost always increase with increasing tempering parameter.

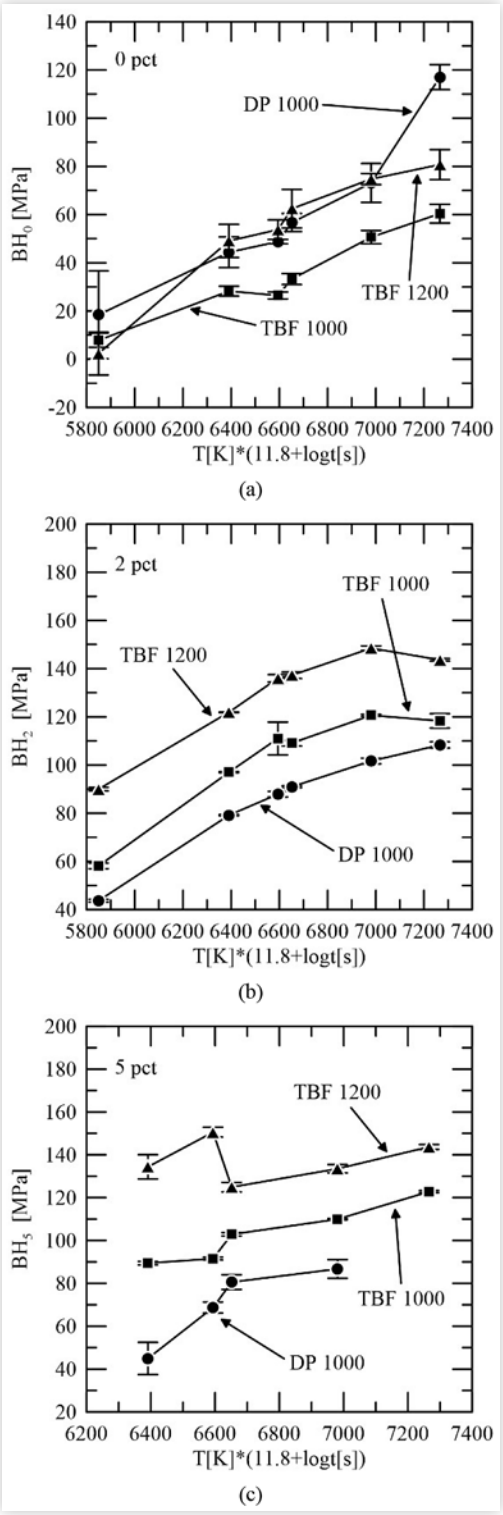

DP 1000 and TBF 1200 showed nearly identical strengthening until the highest tempering parameter corresponding to 200 °C, 60 min. This point is where DP 1000 transitioned from continuous to discontinuous yielding and had the most strengthening for all conditions. Strengthening for DP 1000 reached nearly 120 MPa.

Figures 15(b) and 15(c) show BH_x plotted as a function of tempering parameter for 2 and 5 pct prestrain, respectively. With the addition of prestrain, strengthening response began to separate amongst steels (*i.e.* curves did not overlap). For both 2 and 5 pct prestrain, the most strengthening was always for TBF 1200 and the least for DP 1000. Considering Figure 15(b), both TBF grades appear to reach a maximum at a tempering parameter of 6980, which corresponds to a time/temperature of 200 °C, 15 min. This peak may correspond to overaging, as mentioned by several authors [7, 8, 9,11]. Conversely, DP 1000 continues to increase even at the highest tempering parameter. Figure 15(c) shows that strengthening appears to continuously increase for 5 pct prestrain for all steels. One exception, however, is for TBF 1200 which exhibited a decrease in strengthening for 5 pct prestrain at a low tempering parameter (approximately 6600). Strengthening above this value increased continuously. Regarding DP 1000 with 5 pct prestrain, a large increase was observed at the lowest tempering parameters, then a more gradual increase thereafter which may indicate the beginning of a strengthening plateau. However, only four points are represented for DP 1000 at this prestrain level because {5-200-60} failed outside the extensometer.

Comparing prestrain levels for a single time/temperature, Figure 16 plots BHx as a function of prestrain for DP 1000, TBF 1000, and TBF 1200 baked at 170 °C for 20 min. Without prestrain, DP 1000 and TBF 1200 show the greatest BH0 which is consistent with the observations from Figure 15(a). Increasing prestrain to 2 pct leads to increased BH levels for all grades with the greatest for TBF 1200 and least for DP 1000. Further increasing prestrain leads to a decrease

FIGURE 16 Bake hardening response as a function of prestrain for DP 1000, TBF 1000, and TBF 1200 after baking at 170 °C for 20 min.

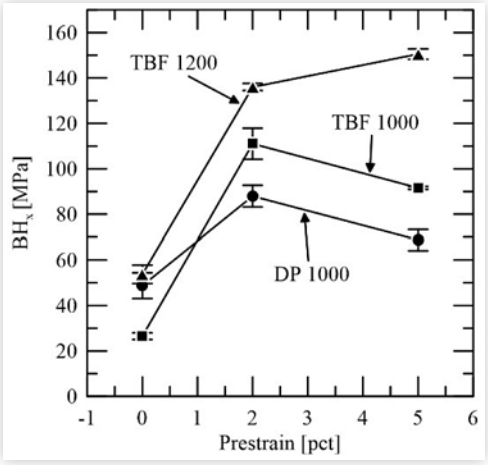

in BH response from DP 1000 and TBF 1000, while TBF 1200 continued to increase. Decrease in BH at higher prestrains has been documented in DP and TBF [7,8,11]. Specifically, in TRIP-type steels, the transformation of retained austenite to martensite at higher prestrain levels, and subsequent tempering during aging, has been correlated with decreases in BH levels [11]. Therefore, the difference in BH response in the two TBF grades at the highest prestrain level may, in part, be attributed to difference in retained austenite stability.

4.4. Significance of Investigation

The objective of this study was to inform automakers - automotive, mechanical, metallurgical engineers, *etc.* - of the significance of paint baking operations on the in-service properties of third generation AHSS. Slight fluctuations in part forming and paint baking operations (changing prestrain, time, or temperature) have been shown to considerably change mechanical properties for the selected experimental steels. It is critical to recognize that bake hardening can lead to added strength but often at the expense of decreased ductility. For example, DP 1000 prestrained 5 pct and baked at 170 °C for 20 min had a YS of 1052 MPa and BH_5 of 69 MPa, but UE decreased to less than 1 pct. Samples baked with no prestrain showed excellent strengthening while retaining tensile ductility, even at the most elevated paint baking condition. All five experimental steels exhibited continuous yielding and YS increases without prestrain. Adding 2 pct prestrain prior to baking also increased strength but decreased ductility for DP and TBF grades.

5. Summary and Conclusions

Tensile tests were performed on five AHSS grades: DP 1000, TBF 1000, TBF 1200, PHS 1500, and PHS 2000. Several prestrain, time, and temperature combinations (Table 2) were tested to evaluate the influence of time, temperature, and prestrain on the BH behavior of these steels. Time and temperature were combined into a single variable, the Hollomon-Jaffe tempering parameter, to make direct comparison of tensile properties possible.

1. Without prestrain, strengthening was observed for DP and TBF steels for all test conditions. Increasing time/temperature lead to increased strengthening up to 200 °C, 60 min. DP 1000 showed the greatest BH response at this time and temperature. Despite increases in YS, UTS remained relatively unchanged for these grades due to minor decreases in strain hardening. Ductility remained high for all test conditions.
2. Tensile testing of PHS grades was limited to unstrained conditions. Differences in BH levels between PHS 1500 and PHS 2000 were attributed to the differences in alloying. Increased carbon in PHS 2000 was responsible for higher dislocation and transition carbide densities, leading to higher strength according to work hardening theory.
3. For both martensitic steels, BH_0 increased to a maximum, then decreased at higher temperatures and longer times. Yielding transitioned from continuous to discontinuous with increasing tempering intensity. The BH response is attributed to the pinning of dislocations by carbon atoms, coarsening of transition carbides, and possible recovery of dislocations. The decrease in BH_0 at higher temperature and longer time conditions may be due to overaging effects.
4. With the addition of 2 and 5 pct prestrain, all grades (excluding PHS 1500 and PHS 2000) showed an increase in yield strength compared to the unstrained conditions and appearance of YPE. Increasing time and temperature (*i.e.* tempering parameter) generally led to higher strength. Plotting BH_x as a function of tempering parameter, TBF 1000 and TBF 1200 samples prestrained 2 pct showed maxima of 121 MPa and 149 MPa, respectively, at 160 °C, 60 min, with subsequent decreases in BH_2 possibly from overaging.
5. As a function of prestrain, the largest BH levels were generally after 2 pct prestrain. One exception was noted for TBF 1200, which showed continually increasing strengthening up to highest tested prestrain level after baking at 170 °C for 20 min. Comparing steel grades, DP 1000 and TBF 1200 exhibited comparable strengthening for the unstrained conditions, while TBF 1000 showed the least strengthening relative to the other two steels. After prestrain (2 and 5 pct), TBF 1200 had the greatest BH values and DP 1000 had the smallest.
6. For DP 1000, TBF 1000, and TBF 1200, ductility was significantly reduced for 2 and 5 pct prestrained samples relative to AR. Tensile elongation generally decreased with increasing time and temperature to a minimum at 200 °C, 60 min. With respect to prestrain, the lowest recorded UE and TE were after 5 pct prestrain for the three steels.
7. For DP and TBF grades, the two measures of strengthening, BH_x and $\Delta\sigma_{max}$, were compared for all time, temperature, and prestrain conditions. TBF 1000 showed good agreement between BH_x and $\Delta\sigma_{max}$, whereas DP 1000 and TBF 1200 exhibited more scattered data. For TBF 1000, work hardening may have contributed more to BH_x, compared to DP 1000 and TBF 1200, considering the generally larger BH_x than $\Delta\sigma_{max}$ for this steel.

References

1. United States Department of Transportation, "2017 and Later Model Year Light-Duty Vehicle Greenhouse Gas Emissions and Corporate Average Fuel Economy Standards," https://www.nhtsa.gov/laws-regulations/corporate-average-fuel-economy, accessed Oct. 2019.
2. Cottrell, A.H. and Bilby, B.A., "Dislocation Theory of Yielding and Strain Ageing of Iron," *Proceedings of the Physical Society* 62(1):49-32, 1949, doi:10.1088/0370-1298/62/1/308.
3. Matlock, D.K., Allen, B.J., and Speer, J.G., "Aging Behavior and Properties of Ultra-Low Carbon Bake-Hardening Steels," *Modern LC and ULC Sheet Steels for Cold Forming: Processing and Properties Conference* 1:265-276, 1998.
4. Waterschoot, T., De, A.K., Vandeputte, S., and De Cooman, B.C., "Static Strain Aging Phenomena in Cold-Rolled Dual Phase Steels," *Metallurgical and Materials Transactions A* 34:781-791, 2003, doi:10.1007/s11661-003-0113-1.
5. Timokhina, I.B., Hodgson, P.D., and Pereloma, E.V., "Transmission Electron Microscopy Characterization of the Bake-Hardening Behavior of Transformation-Induced Plasticity and Dual-Phase Steels," *Metallurgical and Materials Transactions A* 38:2442-2454, 2007, doi:10.1007/s11661-007-9258-7.
6. Timokhina, I.B., Pereloma, E.V., Ringer, S.P., Zheng, R.K. et al., "Characterization of the Bake-Hardening Behavior of Transformation Induced Plasticity and Dual-Phase Steels Using Advanced Analytical Techniques," *ISIJ International* 50(4):574-582, 2010, doi:10.2355/isijinternational.50.574.
7. Gündüz, S., "Static Strain Ageing Behavior of Dual Phase Steels," *Materials Science and Engineering A* 486:63-71, 2008, doi:10.1016/j.msea.2007.08.056.
8. Gündüz, S. and Tosun, A., "Influence of Straining and Ageing on the Room Temperature Mechanical Properties of Dual Phase Steel," *Materials and Design* 29:1914-1918, 2008, doi:10.1016/j.matdes.2008.04.028.
9. Türkmen, M. and Gündüz, S., "Bake-Hardening Response of High Martensite Dual-Phase Steel with Different Morphologies and Volume Fractions," *Acta Metallurgica Sinica* 27(2):279-289, 2014, doi:10.1007/s40195-014-0043-5.
10. Ji, D., Zhang, M., Zhu, D., Luo, S. et al., "Influence of Microstructure and Pre-Straining on the Bake Hardening Response for Ferrite-Martensite Dual-Phase Steels of Different Grades," *Material Science and Engineering A* 708:129-141, 2017, doi:10.1016/j.msea.2017.09.127.
11. Ramazani, A., Bruehl, S., Gerber, T., Bleck, W. et al., "Quantification of Bake Hardening Effect in DP600 and TRIP700 Steels," *Materials and Design* 57:479-486, 2014, doi:10.1016/j.matdes.2014.01.001.
12. Samek, L., De Moor, E., Penning, J., Speer, J.G. et al., "Static Strain Aging of Microstructural Constituents in Transformation-Induced-Plasticity Steel," *Metallurgical and Materials Transactions A* 39(11):2542-2554, 2008, doi:10.1007/s11661-008-9605-3.
13. Zhang, L.C., Timokhina, I.B., La Fontaine, A., Ringer, S.P. et al., "Effect of Pre-Straining and Bake Hardening on the Microstructure and Mechanical Properties of CMnSi TRIP Steels," *La Metallurgia Italiana* 49-55, 2009.
14. Das, S., Timokhina, I., Singh, S.B., Pereloma, E. et al., "Effect of Bainitic Transformation on Bake Hardening in TRIP Assisted Steel," *Materials Science and Engineering A* 534:485-494, 2012, doi:10.1016/j.msea.2011.11.097.
15. Neugebauer, R., Schieck, F., Polster, S., Mosel, A. et al., "Press Hardening - An Innovative and Challenging Technology," *Archives of Civil and Mechanical Engineering* 12:113-118, 2012, doi:10.1016/j.acme.2012.04.013.
16. Naganathan, A. and Penter, L., *Sheet Metal Forming - Processes and Applications* (Materials Park: ASM International, 2012), 133-142. ISBN:978-1-61503-844-2.
17. Krauss, G., *Steels - Processing, Structure, and Performance, Second Edition* (Materials Park: ASM International, 2015), 414-425. ISBN:978-1-62708-083-5.
18. "Standard Test Methods for Tension Testing of Metallic Materials," ASTM Standard E8/E8M-16a, 2016.
19. Leslie, W.C., *The Physical Metallurgy of Steel, First Edition* (New York: McGraw-Hill, 1981), 79-91. ISBN:0-07-037780-4.
20. Dieter, G.E., *Mechanical Metallurgy, Third Edition* (New York: McGraw-Hill, 1986), 197-203. ISBN:0-07-016893-8.
21. Hollomon, J.H. and Jaffe, L.D., "Time-Temperature Relations in Tempering Steel," *Metals Technology* 1831:1-26, 1945.
22. Leslie, W.C., *The Physical Metallurgy of Steels, First Edition* (New York: McGraw-Hill, 1981), 38-43. ISBN:0-07-037780-4.
23. Nutor, R.K., Adomako, N.K., and Fang, Y.Z., "Using the Hollomon Model to Predict Strain-Hardening in Metals," *American Journal of Materials Synthesis and Processing* 2(1):1-4, 2017, doi:10.11648/j.ajmsp.20170201.11.
24. Ludwik, P., *Element der Technologischen Mechanik* (Berlin: Springer, 1909), 268. ISBN:978-3-662-39265-2.
25. Jaoul, B., "Etude de la Forme des Courbes de Deformation Plastique," *Journal of Mechanics and Physics of Solids* 5:95-114, 1957, doi:10.1016/0022-5096(57)90054-6.
26. Speich, G. and Leslie, W.C., "Tempering of Steel," *Metallurgical Transactions* 3(5):1043-1054, 1972, doi:10.1007/BF02642436.
27. Saeglitz, M. and Krauss, G., "Deformation, Fracture, and Mechanical Properties of Low-Temperature-Tempered Martensite in SAE 43xx Steels," *Metallurgical and Materials Transactions A* 28(2):377-387, 1997, doi:10.1007/s11661-997-0139-x.
28. Kuhlmann-Wilsdorf, D., "Theory of Workhardening 1934-1984," *Metallurgical Transactions A* 16(12):2091-2108, 1985, doi:10.1007/BF02670414.
29. Dieter, G.E., *Mechanical Metallurgy, Third Edition* (New York: McGraw-Hill, 1986), 139-144. ISBN:0-07-016893-8.

Contact Information

B.W. Blesi, bwbwyo@hotmail.com; **Emmanuel De Moor**, edemoor@mines.edu, 303-273-3624. Advanced Steel Processing and Products Research Center, Colorado School of Mines, Golden, CO, 80401, USA.

Acknowledgments

The authors gratefully acknowledge the support of the sponsors of the Advanced Steel Processing and Products Research Center, an industry/university cooperative research center at the Colorado School of Mines. The authors recognize ArcelorMittal, Gestamp, and voestalpine for supplying the material for this project. B.W. Blesi would like to thank the Department of Defense's Science, Mathematics, and Research for Transformation (SMART) Scholarship program for supporting his time at Colorado School of Mines.

ISSN 0148-7191